

# Shallow-band superconductors: pushing superconductivity types apart

S. Wolf,<sup>1</sup> A. Vagov,<sup>1</sup> A. A. Shanenkov,<sup>2</sup> V. M. Axt,<sup>1</sup> and J. Albino Aguiar<sup>2</sup>

<sup>1</sup>*Institut für Theoretische Physik III, Bayreuth Universität, Bayreuth, Germany*

<sup>2</sup>*Departamento de Física, Universidade Federal de Pernambuco, Recife, PE, Brazil*

(Dated: March 10, 2021)

Magnetic response is a fundamental property of superconducting materials, which helps to distinguish two superconductivity types: the ideally diamagnetic type I and type II, which can develop the mixed state with Abrikosov vortices. We demonstrate that multi-band superconductors with one shallow band, that have recently attracted much attention for their high critical temperatures and unusual properties, often stay apart of this simple classification. In a wide range of microscopic parameters such systems fall into the inter-type or transitional interval in between the standard types and display unconventional mixed state configurations.

The ongoing search for superconductors with higher transition temperatures ignited intense research on materials with many carrier bands (multi-band systems) with so-called shallow bands [1]. It has long been known that superconductivity properties in multi-band materials are very sensitive to the position of the chemical potential. As was first predicted in 1970's if a chemical potential touches the lowest energy point of a band with a large density of states (DOS) the superconductivity may enter the regime of the BCS-BEC crossover [2]. Evidences of this regime have been recently observed in multi-band FeSe<sub>x</sub>Te<sub>1-x</sub> [3]. However, the research on the role of shallow bands is, at present, limited to a few microscopic characteristics of the BCS-BEC crossover, such as increased fluctuations and the appearance of the pseudogap (for recent developments see [4, 5] and references therein). Until now, manifestations of the BCS-BEC crossover on a macroscopic level, in particular possible modifications of the magnetic properties, remain largely unknown. In this Letter we demonstrate that many multi-band superconductors with a shallow band are in a mixed state and reveal magnetic properties that cannot be attributed to standard superconductivity types.

We start by recalling the well known fact that the Ginzburg-Landau (GL) theory predicts that the magnetic response of a superconductor is determined by the GL parameter  $\kappa = \lambda/\xi$ , where  $\lambda$  is the magnetic penetration depth and  $\xi$  is the GL coherence length [6–8]. The superconductivity types interchange sharply at the critical GL parameter  $\kappa_0 = 1/\sqrt{2}$ , so that at  $\kappa < \kappa_0$  or  $\kappa > \kappa_0$  a superconductor belongs, respectively, to type I or II. More elaborate theoretical analysis [9] as well as experimental studies [10–13] have led to the conclusion that the type interchange takes place over a finite interval of  $\kappa$ 's, here referred to as *inter-type interval* or *inter-type domain*, if considered in the entire  $(\kappa, T)$ -plane. In conventional single-band materials this domain is narrow and is usually ignored in most discussions of the superconductivity types. Superconductivity properties in this interval are investigated in detail neither theoretically nor experimentally. The studies presented so far suggest that it has many non-conventional phenomena, not found in stan-

dard bulk superconductors. In particular, unlike type II materials such inter-type superconductors demonstrate the first order first-order phase transition between the Meissner and the mixed states, which is associated with non-monotonic vortex-vortex interactions [14] (schematic magnetization curves are shown in Fig. 1). They also demonstrate stable multi-quantum vortices [15, 16] and a giant paramagnetic Meissner effect [17].

In this work, using a two-band prototype model of a superconductor, we demonstrate that the presence of a shallow band with strong pairing interaction dramatically enlarges the inter-type domain and thus changes qualitatively the magnetic properties of such systems. To this end we study details of the interchange of superconductivity types. A standard description of the interchange in the GL theory is done by introducing a critical GL parameter  $\kappa^*$ , which marks the appearance of the mixed state at the thermodynamic critical field  $H_c$ , so that at  $\kappa > \kappa^*$  it wins energetically over the uniform Meissner state. It is obtained by solving the equation:

$$\mathfrak{G}(\kappa^*, T) = 0, \quad \mathfrak{G} = \int \mathfrak{g} \, d\mathbf{r}, \quad \mathfrak{g} = \mathfrak{f} + \frac{H_c^2}{8\pi} - \frac{H_c B}{4\pi} \quad (1)$$

where  $\mathfrak{G}$  is the Gibbs energy difference between the mixed and the Meissner states calculated at  $H_c$  and  $\mathfrak{f}$  is the condensate free-energy density. The magnetic induction  $\mathbf{B}$  is assumed parallel to the external field  $H = H_c$ .

In the GL theory a particular choice of the non-uniform mixed state is not important for criterion (1): one obtains the same critical parameter  $\kappa^* = \kappa_0$  for all possible flux configurations. The reason is a special degeneracy of the GL equations at  $\kappa_0$ , often referred to as the Bogomolny point [18]. However, beyond the GL theory at  $T < T_c$  this degeneracy is removed and  $\kappa^* = \kappa_i^*$  depends on the flux configuration  $i$ . The number of topologically different configurations  $i$  is infinite and so is the number of critical parameters  $\kappa_i^*$ . This defines a finite inter-type interval  $[\kappa_{min}^*, \kappa_{max}^*]$ , where superconductivity types interchange gradually by a sequential appearance of flux configurations  $i$  when  $\kappa_i^*$  is crossed. Previous research indicates that the lower boundary of this interval is defined by the start of superconductivity nucleation at  $H_c$

(this is equivalent to the condition  $H_{c2} = H_c$ ), while the upper boundary is determined by the appearance of a long-range attraction between two Abrikosov vortices.

We now calculate the inter-type boundaries for a model with two carrier bands, one of which is a shallow 2D band with a minimal energy that coincides with the chemical potential. The lower dimensionality of the band increases its DOS, which is crucial for reaching the BCS-BEC crossover regime [19]. The other band is deep. Its dimensionality is not so important, although a 2D model requires more attention in view of thermal fluctuations. However, once it is assumed that the superconductivity in the deep band can be described within the mean field approach, details of the model are not critical. For simplicity we assume that both bands are two dimensional.

According to the BCS theory the free-energy density of the condensate state in a two-band system writes as:

$$\mathfrak{f} = \frac{\mathbf{B}^2}{8\pi} + \Delta^\dagger \check{g}^{-1} \Delta + \sum_{\nu=1,2} \mathfrak{f}_\nu, \quad (2)$$

where  $\Delta^\dagger = (\Delta_1^*(\mathbf{r}), \Delta_2^*(\mathbf{r}))$  is the band gap function and  $\check{g}^{-1}$  is the inverted  $2 \times 2$  coupling matrix with real  $g_{ij} = g_{ji}$ . We calculate the free energy using the perturbation expansion with the small parameter  $\tau = 1 - T/T_c$ , which leads to the so-called extended GL (EGL) theory [20, 21]. For a two-band system the lowest order of the expansion yields the standard GL theory with a single order parameter [21, 22]. A far-reaching consequence of this fact is that two-band superconductors follow the standard classification, where types I and II are separated by the Bogomolny point at  $T_c$  and by a finite inter-type interval at  $T < T_c$ .

The perturbation expansion is derived similarly to Ref. [21], with the difference that here the bands are qualitatively different (shallow and deep), which leads to additional contributions to the series expansion. Here, we present a sketch of the derivation which highlights the differences with Ref. [21]. Expanding  $\mathfrak{f}_\nu$  in Eq. (2) in powers of  $\Delta_\nu$  and its gradients yields:

$$\begin{aligned} \mathfrak{f}_\nu = & -a_{1,\nu} |\Delta_\nu|^2 + a_{2,\nu} |\mathbf{D}\Delta_\nu|^2 - a_{3,\nu} \left( |\mathbf{D}^2 \Delta_\nu|^2 \right. \\ & + \frac{\text{rot} \mathbf{B} \cdot \mathbf{i}_\nu}{3} + \frac{4e^2}{\hbar^2 c^2} \mathbf{B}^2 |\Delta_\nu|^2 \Big) + a_{4,\nu} \mathbf{B}^2 |\Delta_\nu|^2 \\ & + \frac{b_{1,\nu}}{2} |\Delta_\nu|^4 - \frac{b_{2,\nu}}{2} \left( L_\nu |\Delta_\nu|^2 |\mathbf{D}\Delta_\nu|^2 \right. \\ & \left. + l_\nu [(\Delta_\nu^*)^2 (\mathbf{D}\Delta_\nu)^2 + \text{c.c.}] \right) - \frac{c_{1,\nu}}{3} |\Delta_\nu|^6, \end{aligned} \quad (3)$$

where the band coefficients  $a_{n,\nu}$ ,  $b_{n,\nu}$ ,  $c_{n,\nu}$  are  $T$ -dependent. The constants  $L_\nu$  and  $l_\nu$  are introduced to capture the differences between the bands and

$$\mathbf{i}_\nu = \frac{4e}{\hbar c} \text{Im}[\Delta_\nu \mathbf{D}^* \Delta_\nu^*], \quad \mathbf{D} = \nabla - \frac{i2e}{\hbar c} \mathbf{A}. \quad (4)$$

The  $\tau$ -expansion is obtained by representing all quantities in Eq. (3) as  $\tau$ -series:

$$\begin{aligned} \Delta_\nu &= \tau^{1/2} [\Delta_\nu^{(0)} + \tau \Delta_\nu^{(1)}], \quad \mathbf{A} = \tau^{1/2} [\mathbf{A}^{(0)} + \tau \mathbf{A}^{(1)}], \\ \mathbf{B} &= \tau [\mathbf{B}^{(0)} + \tau \mathbf{B}^{(1)}], \quad H_c = \tau [H_c^{(0)} + \tau H_c^{(1)}], \end{aligned} \quad (5)$$

where the two lowest orders, needed to derive the leading order corrections to the GL theory, are kept. We take into account the  $\tau$ -scaling of the coordinates [20], which introduces an additional factor  $\sqrt{\tau}$  for each gradient in the series. Expanding the temperature-dependent coefficients in Eq. (3) yields:

$$\begin{aligned} a_{1,\nu} &= \mathcal{A}_\nu - \tau [a_\nu^{(0)} + \tau a_\nu^{(1)}], \quad a_{2,\nu} = \mathcal{K}_\nu^{(0)} + \tau \mathcal{K}_\nu^{(1)}, \\ a_{3,\nu} &= \mathcal{Q}_\nu^{(0)}, \quad a_{4,\nu} = r_\nu^{(0)}, \quad b_{1,\nu} = b_\nu^{(0)} + \tau b_\nu^{(1)}, \\ b_{2,\nu} L_\nu &= \mathcal{L}_\nu^{(0)}, \quad b_{2,\nu} l_\nu = \ell_\nu^{(0)}, \quad c_{1,\nu} = c_\nu^{(0)}, \end{aligned} \quad (6)$$

where the coefficients are calculated from the chosen microscopic model for the band states. Substituting Eqs. (5), (6) and the gradient scaling into Eq. (3) and then calculating the integrals in Eq. (1) one derives the  $\tau$ -expansion for  $\mathfrak{G}$ .

It is important that the leading correction to the GL free energy requires only  $\Delta_{1,2}^{(0)}$  and  $\mathbf{B}^{(0)}$  while  $\Delta_{1,2}^{(1)}$  and  $\mathbf{B}^{(1)}$  are not needed [21]. Thus, the corrected free energy can be evaluated from the knowledge of the solution of the GL equations alone. The latter exhibits a single order parameter  $\Psi$ , which determines both gaps by:

$$\begin{pmatrix} \Delta_1^{(0)} \\ \Delta_2^{(0)} \end{pmatrix} = \begin{pmatrix} S^{-1/2} \\ S^{1/2} \end{pmatrix} \Psi(\mathbf{r}). \quad (7)$$

The band weight factor  $S$  is obtained by solving the linearized gap equation for  $T_c$  which yields:

$$S = \frac{1}{g_{12}} (g_{22} - G \mathcal{A}_1) = \frac{g_{12}}{g_{11} - G \mathcal{A}_2}, \quad (8)$$

where  $G = \det[g] = g_{11}g_{22} - g_{12}^2$ . The integration in Eq. (1) is simplified with the help of the GL equations and the final result for  $\mathfrak{G}$  depends only on the integrals:

$$\mathcal{I} = \int |\Psi|^2 (1 - |\Psi|^2) d\mathbf{r}, \quad \mathcal{J} = \int |\Psi|^4 (1 - |\Psi|^2) d\mathbf{r}. \quad (9)$$

Solving Eq. (1) up to the leading order corrections of the GL theory we obtain:

$$\kappa^* = \kappa_0 + \tau \kappa^{*(1)} \quad (10)$$

with

$$\begin{aligned} \frac{\kappa^{*(1)}}{\kappa_0} &= \bar{\mathcal{K}} - \bar{c} + 2\bar{\mathcal{Q}} + \bar{G} \bar{\beta} (2\bar{\alpha} - \bar{\beta}) \\ &+ \frac{\mathcal{J}}{\mathcal{I}} \left( \frac{\bar{\mathcal{L}}}{4} - \bar{c} - \frac{5}{3} \bar{\mathcal{Q}} - \bar{G} \bar{\beta}^2 \right), \end{aligned} \quad (11)$$

$\nu$	$\mathcal{M}_{b,\nu}^{(0)}$	$\mathcal{M}_{c,\nu}^{(0)}$	$\mathcal{M}_{\mathcal{K},\nu}^{(0)}$	$\mathcal{M}_{\mathcal{Q},\nu}^{(0)}$	$\mathcal{M}_{\mathcal{L},\nu}^{(0)}$	$\mathcal{M}_{a,\nu}^{(1)}$	$\mathcal{M}_{b,\nu}^{(1)}$	$\mathcal{M}_{\mathcal{K},\nu}^{(1)}$
1	$7\zeta(3)/(8\pi^2)$	$93\zeta(5)/(128\pi^4)$	$7\zeta(3)/(32\pi^2)$	$93\zeta(5)/(2048\pi^4)$	$31\zeta(5)/(32\pi^4)$	1/2	2	2
2	$7\zeta(3)/(8\pi^2)$	$93\zeta(5)/(128\pi^4)$	$3\zeta(2)/(8\pi^2)$	$7\zeta(3)/(512\pi^2)$	$25\zeta(4)/(16\pi^4)$	1/2	2	1

TABLE I. Numerical factors  $\mathcal{M}_{w,\nu}^{(0)}$  (with  $w = b, c, \mathcal{K}, \mathcal{Q}, \mathcal{L}$ ) and  $\mathcal{M}_{w,\nu}^{(1)}$  (with  $w = a, b, \mathcal{K}$ ) for the deep ( $\nu = 1$ ) and shallow ( $\nu = 2$ ) bands, see Eqs. (14) and (15). In the table  $\zeta(x)$  is the Riemann zeta function of  $x$ .

where the dimensionless constants read as:

$$\begin{aligned}\bar{\mathcal{K}} &= \frac{\mathcal{K}^{(1)}}{\mathcal{K}} - \frac{b^{(1)}}{2b}, \quad \bar{c} = \frac{ca}{3b^2}, \quad \bar{\mathcal{Q}} = \frac{a\mathcal{Q}}{\mathcal{K}^2}, \quad \bar{\mathcal{L}} = \frac{a\mathcal{L}}{b\mathcal{K}}, \\ \bar{G} &= \frac{Ga}{4g_{12}}, \quad \bar{\alpha} = \frac{\alpha}{a} - \frac{\Gamma}{\mathcal{K}}, \quad \bar{\beta} = \frac{\beta}{b} - \frac{\Gamma}{\mathcal{K}}.\end{aligned}\quad (12)$$

The coefficients are defined by the band contributions as:

$$\begin{aligned}\omega &= \frac{\omega_1^{(0)}}{S^p} + S^p w_2^{(0)}, \quad \omega^{(1)} = \frac{\omega_1^{(1)}}{S^p} + S^p w_2^{(1)}, \\ \alpha &= \frac{a_1^{(0)}}{S} - S a_2^{(0)}, \quad \beta = \frac{b_1^{(0)}}{S^2} - S^2 b_2^{(0)}, \\ \Gamma &= \frac{\mathcal{K}_1^{(0)}}{S} - S \mathcal{K}_2^{(0)}.\end{aligned}\quad (13)$$

where  $\omega = \{a, \mathcal{K}, \mathcal{Q}, r, b, \mathcal{L}, c\}$ ,  $\omega^{(1)} = \{\mathcal{K}^{(1)}, b^{(1)}\}$ ,  $w_\nu^{(0)} = \{a_\nu^{(0)}, \mathcal{K}_\nu^{(0)}, \mathcal{Q}_\nu^{(0)}, r_\nu^{(0)}, b_\nu^{(0)}, \mathcal{L}_\nu^{(0)}, c_\nu^{(0)}\}$  and values  $p = \{1, 2, 3\}$  appear respectively for coefficients  $a_{n,\nu}$ ,  $b_{n,\nu}$  and  $c_{n,\nu}$ .

The band coefficients in Eq. (6) are calculated for a model with 2D quadratic dispersion for both bands. We note that in the EGL formalism the band dimensionality affects the results mainly via the ratio between the band DOSs. The calculations are done in the clean limit. For the deep band ( $\nu = 1$ ) the inequality  $\Delta_1 \ll \mu - \varepsilon_{1,k=0}$  means that we can use standard approximations employed in the derivations of the EGL theory for the 3D case [20]. For the shallow band ( $\nu = 2$ ) the chemical potential is assumed to coincide with the band minimum,  $\mu = \varepsilon_{2,k=0}$ . Then the leading order coefficients in Eq. (6) are:

$$\begin{aligned}\mathcal{A}_\nu &= N_\nu \ln \left( \frac{2e^\gamma \hbar \omega_c}{\pi T_c} \right), \quad a_\nu^{(0)} = -N_\nu, \quad b_\nu^{(0)} = N_\nu \frac{\mathcal{M}_{b,\nu}^{(0)}}{T_c^2}, \\ c_\nu^{(0)} &= N_\nu \frac{\mathcal{M}_{c,\nu}^{(0)}}{T_c^4}, \quad \mathcal{K}_\nu^{(0)} = N_\nu \mathcal{M}_{\mathcal{K},\nu}^{(0)} \frac{\hbar^2 v_\nu^2}{T_c^2}, \\ \mathcal{Q}_\nu^{(0)} &= N_\nu \mathcal{M}_{\mathcal{Q},\nu}^{(0)} \frac{\hbar^4 v_\nu^4}{T_c^4}, \quad \mathcal{L}_\nu^{(0)} = N_\nu \mathcal{M}_{\mathcal{L},\nu}^{(0)} \frac{\hbar^2 v_\nu^2}{T_c^4},\end{aligned}\quad (14)$$

where  $\hbar \omega_c$  is the cut-off energy,  $\gamma$  is the Euler constant,  $N_\nu$  is the band DOS,  $v_\nu$  denotes the characteristic band velocity, i.e., the Fermi velocity  $v_F = \sqrt{2\mu/m_\nu}$  for the deep band and the temperature velocity  $v_T = \sqrt{2T_c/m_\nu}$  for the shallow band. The additional numerical factors  $\mathcal{M}_{w,\nu}^{(0,1)}$  are listed in Tab. I. The band DOSs are

$N_\nu = \tilde{N}_\nu m_\nu / (2\pi \hbar^2)$  with  $\tilde{N}_\nu$  being an additional factor that accounts for the density of states in z-direction (this quantity accounts for the 3D character of the entire system and does not affect the final conclusions). The next-order coefficients in Eq. (6) are given by:

$$w_\nu^{(1)} = \mathcal{M}_{w,\nu}^{(1)} w_\nu^{(0)}, \quad (15)$$

where  $w = \{a, \mathcal{K}, b\}$ .

Knowing the ratio  $\eta = N_2/N_1$  of the DOSs and the coupling constants  $\lambda_{ij} = g_{ij}N$  ( $N = N_1 + N_2$ ) one obtains the critical temperature  $T_c$  from the linearized gap equation and then  $\kappa^*$  from Eq. (11). It is important that apart from  $T_c$  the final expression for  $\kappa^*$  depends only on  $\eta$  and  $v_2/v_1$ , but not on  $N_{1,2}$  and  $v_{1,2}$  separately. The ratio  $\mathcal{J}/\mathcal{I}$  in Eq. (11) is calculated using the solution of the GL equations at  $\kappa_0$ , which at this point reduces to the pair of self-dual Sarma-Bogomolny equations [6, 18].

As mentioned before, the lowest boundary of the inter-type interval  $\kappa_{min}^*$  is calculated from the condition that the inhomogeneous mixed state disappears at  $H_c$ . It follows from Eq. (9) that in the limit of a vanishing mixed state one has  $\mathcal{J}/\mathcal{I} = 0$ . The upper boundary  $\kappa_{max}^*$  is defined by the condition that the sign in the long-range vortex-vortex interaction changes. In this case we need to calculate the long-range asymptote of  $\mathcal{J}(R)/\mathcal{I}(R)$  for the two-vortex solution as a function of the distance  $R$  between the vortices. This can be done analytically yielding the exact asymptote  $\mathcal{J}(R)/\mathcal{I}(R) = 2$  at  $R \rightarrow \infty$ .

Although the final expression for  $\kappa^*$  is a complicated algebraic function of the microscopic model parameters, it can be considerably simplified for the case of a two-band system with  $v_2/v_1 \sim \sqrt{T_c/\mu} \ll 1$  in the vicinity of the BCS-BEC crossover, where the contribution of the shallow band to the condensate state is dominant and thus  $S \gtrsim 1$  in Eq. (8) [19]. We obtain:

$$\frac{\kappa^{(1)*}}{\kappa_0} \approx \tilde{\mathcal{Q}} \left( 2 - \frac{5}{3} \frac{\mathcal{J}}{\mathcal{I}} \right) S^2 \eta, \quad \tilde{\mathcal{Q}} = \frac{a_1^{(0)} \mathcal{Q}_1^{(0)}}{\mathcal{K}_1^{(0)2}}, \quad (16)$$

where the bracket gives 2 for  $\kappa_2^*$  and  $-4/3$  for  $\kappa_{li}^*$ , if we use the above results for the  $\mathcal{J}/\mathcal{I}$  ratio. According to this simplified expression the width of the inter-type domain is governed by the ratio of the DOSs  $\eta$ , the couplings (via  $S$ ) and the dimensionless constant  $\tilde{\mathcal{Q}}$ . Equations (3) and (6) show that  $\tilde{\mathcal{Q}}$  controls the contribution of the fourth-

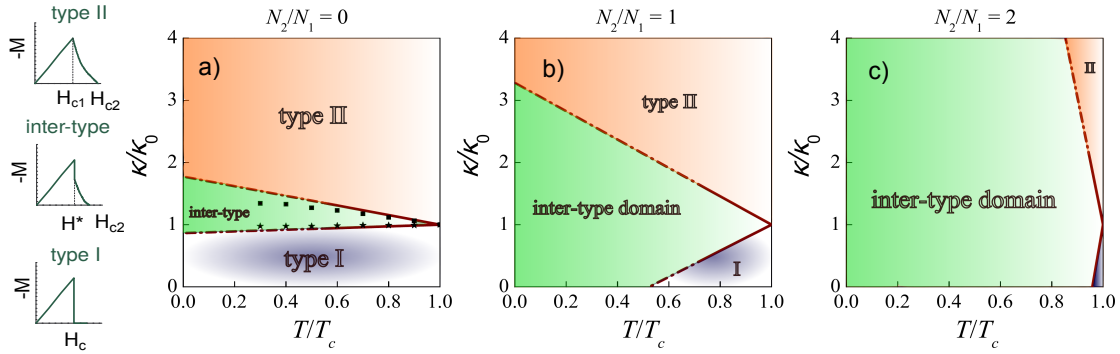


FIG. 1. Phase diagram of a two-band superconductor on the  $(\kappa, T)$ -plane. The left panels illustrates schematically the magnetization field dependence of types I and II and of the inter-type domain. Panels a), b) and c) correspond to  $\eta = 0, 1$  and  $2$ , respectively, demonstrating progressive widening of the inter-type domain. For comparison, dots in the left panel represent numerical results for the inter-type boundaries (squares for  $\kappa_{max}^* = \kappa_{li}^*$  and stars for  $\kappa_{min}^* = \kappa_2^*$ ), obtained by solving the Eilenberger equation [23].

order gradient term in the free-energy expansion for the deep band.

Taking into account that  $S$  increases with  $\eta$ , when the system is close to the crossover [19], one concludes that the inter-type interval increases with  $\eta$ . This widening of the inter-type domain in the  $(\kappa, T)$ -plane is illustrated in Fig. 1, where three panels show  $\kappa_2^*$  and  $\kappa_{li}^*$  as functions of temperature (this is of course a linear dependence in the EGL theory) calculated at  $\eta = 0, 1, 2$  using the non-simplified expressions for  $\kappa^*$ . We note that  $\kappa^*$  depends only modestly on the coupling constants but is indeed very sensitive to the value of  $\eta$ . We also note that when  $\eta = 0$  (left panel) only the deep band is involved in the condensate formation so that our results should be comparable with those obtained earlier for a single-band model. Indeed, a comparison with microscopic numerical calculations for a 2D system [23], shown by dots in the left panel of Fig. 1, reveals a very good quantitative agreement down to temperatures  $0.5T_c$ . At larger  $\eta$  the contribution of the shallow band to the condensate increases and the inter-type domain widens sharply, as shown in the middle and right panels of Fig. 1.

We now address the question whether thermal fluctuations invalidate the mean field foundations of the GL and EGL approaches. It is well known that the existence of shallow bands strongly enhances fluctuations. This can be seen by considering the fluctuation-related contribution to the heat capacity. The GL theory for a single-band system yields for this quantity  $\delta C_V \sim (L/\xi_0)^2 \tau^{-1}$ , where  $L$  is the sample length and  $\xi_0^2 = -\mathcal{K}/a$  is the zero-temperature GL coherence length [8]. Here, this length is determined by the coefficients of the GL equation, but it is also related to the microscopic BCS coherence length or the Cooper-pair size. One notices that the coherence length calculated separately for the shallow band,  $\xi_{0,2} \sim v_2$ , is rather small and, therefore, the corresponding Ginzburg-Levanjuk parameter  $Gi_2$  (temperature interval around  $T_c$ , where the fluctuations in this band are important) may become comparable with

the temperature interval where the EGL theory can be used. However, in a two-band system the fluctuations are screened due to the interactions with the deep band. This follows from the calculations of the full two-band coherence length, which yields  $\xi_0^2 = \sum_\nu \rho_\nu \xi_{0,\nu}^2$  with  $\rho_\nu$  being the band weight factors. The large coherence length of the deep band,  $\xi_{0,1}$ , ensures that  $\xi_0$  is not very small (unless  $\rho_1 \ll \rho_2$ ). In the same limit, that was used to derive Eq. (16), one obtains  $\xi_0 \approx \xi_{0,1}/(S\sqrt{\eta})$  as an estimation for the coherence length and  $Gi \approx Gi_1 S^2 \eta$  for the corresponding Ginzburg-Levanjuk parameter of the two-band system, where  $Gi_1$  is this quantity calculated separately for the deep band. Thus, the enlargement of the inter-type domain in Eq. (16) and the increase of  $Gi$  is controlled by the same factor  $S^2 \eta$ . One concludes that a notable enlargement of the inter-type domain can be achieved without compromising the validity of the mean field calculations if  $Gi_1$  is small enough. We also note that the above relations suggest an interesting inverse dependence  $\kappa_{li}^* - \kappa_2^* \propto \xi_0^{-2}$  of the inter-type interval on the correlation length, or the Cooper-pair size,  $\xi_0$ .

In summary we predict that the inter-type domain between the two standard superconductivity types is considerably enlarged in multi-band materials with a shallow band when the latter yields a measurable contribution to the condensate state. Thus for a wide range of microscopic parameters a multi-band superconductor can fall into this domain. This will reveal itself in many notable changes in the system's magnetic properties, which resemble the type I or II superconductivity only in the close vicinity of the critical temperature  $T_c$ . At lower temperatures such superconductors enter the inter-type domain. Although a comprehensive description of the inter-type domain has not been achieved yet it is possible to predict that the mixed state in such systems will exhibit many unusual spatial vortex configurations not observed in standard type II superconductors.

The work was supported by Brazilian CNPq (grants 307552/2012-8 and 141911/2012-3) and FACEPE (grant

APQ-0589-1.05/08).

- 
- [1] I. Bozovic and C. Ahn, Nat. Phys. **10**, 892 (2014).
  - [2] D. M. Eagles, Phys. Rev. **186**, 456 (1969).
  - [3] Y. Lubashevsky, E. Lahoud, K. Chashka, D. Podolsky, and A. Kanigel, Nat. Phys. **8**, 30 (2012).
  - [4] I. Bloch, J. Dalibard, and W. Zwerger, Rev. Mod. Phys. **80**, 885 (2008).
  - [5] J. P. Gaebler, J. T. Stewart, T. E. Drake, D. S. Jin, A. Perali, P. Pieri, and G. C. Strinati, Nat. Phys. **6**, 569 (2010).
  - [6] P. G. de Gennes, *Superconductivity of Metals and Alloys*, (Benjamin, New York, 1966).
  - [7] E. M. Lifshitz and L. P. Pitaevskii, *Statistical Physics, Part 2, Course of Theoretical Physics*, Vol. 9 (Oxford, Pergamon, 1980).
  - [8] Ketterson, J. B. & Song, S. N. *Superconductivity* (Univ. Press, Cambridge, 1999).
  - [9] A. E. Jacobs, Phys. Rev. B **4**, 3022 (1971).
  - [10] U. Krägeloh, Phys. Lett. A **28**, 657 (1969).
  - [11] U. Essmann, Physica **55**, 83 (1971).
  - [12] D. R. Aston, R. L. W. Dubeck, and F. Rothwarf, Phys. Rev. B **3**, 2231 (1971).
  - [13] J. Auer and H. Ullmaier, Phys. Rev. B **7**, 136 (1973).
  - [14] A. E. Jacobs, Phys. Rev. B **4**, 3029 (1971).
  - [15] G. Lasher, Phys. Rev. **154**, 345 (1967).
  - [16] Yu. N. Ovchinnikov, JETP **88**, 398 (1988) [Zh. Eksp. Teor. Fiz. **115**, 726 (1988), in Russian].
  - [17] R. M. da Silva, M. V. Milošević, A. A. Shanenko, F. M. Peeters, and J. Albino Aguiar, Sci. Rep. **5**, 12695 (2015).
  - [18] E. B. Bogomolnyi, Sov. J. Nucl. Phys. **24**, 449 (1976).
  - [19] A. A. Shanenko, M. D. Croitoru, A. V. Vagov, V. M. Axt, A. Perali, and F. M. Peeters, Phys. Rev. A **86**, 033612 (2012).
  - [20] A. A. Shanenko, M. V. Milošević, F. M. Peeters, and A. Vagov, Phys. Rev. Lett. **106**, 047005 (2011).
  - [21] A. Vagov, A. A. Shanenko, M. V. Milošević, V. M. Axt, F. M. Peeters, Phys. Rev. B **85**, 014502 (2012).
  - [22] V. G. Kogan and J. Schmalian, Phys. Rev. B **83**, 054515 (2011).
  - [23] P. Miranović and K. Machida, Phys. Rev. B **67**, 092506 (2003).